Morphological and mineralogical characterization of Cavalerius crater in the equatorial transition region of moon

Nidhi Roy, Priyadarshini Singh, Deepali Singh, Vikas Rena and Saumitra Mukherjee*

School of Environmental Sciences, Jawaharlal Nehru University, New Delhi, 110 067, India

ABSTRACT

The crater in the equatorial transition region represents unique morphological and mineralogical features. Cavalerius crater lying in the transition region centred at 5.1°N and 66.8°W highlights the features of both mare and highland region. The morphology of the crater was studied using High resolution data of Narrow Angle Camera (NAC) and Wide angle Camera (WAC) onboard Lunar Reconnaissance Orbiter. The study highlights the presence of two irregular central mounds, wall terraces, slumped wall formed due to landslide features, smooth floor units and hummocky units within the crater. Further, crater profile study is carried out using Lunar Orbiter Laser Altimeter (LOLA) dataset to figure out the crater rim-floor elevation, Central mound elevation and distance between the terraces and closest rim. The mineralogical study using Chandrayaan-1 Moon mineralogy mapper and Clementine dataset concludes the crater floor to be rich in clinopyroxene and olivine while the inner and outer rim had abundance of orthopyroxene. The study emphasizes the unique morphology and mineral availability within the crater.

Key words: *Cavalerius Crater, Morphology, Mineralogy, Transition region, Central mound.*

Introduction

Craters on moon represent the unique morphological and mineralogical characteristics. It is widely distributed in the near and far-side of the surface of moon (Arivazhagan *et al.,* 2018). Craters have been divided into simple and complex craters with reference to geometry. Simple craters are bowl shaped circular depressions with smooth rims lacking terraces and flat crater floor (Heiken *et al.,* 1991). Complex craters are characterised by uplifted central peak, flat floors, rims having terraced walls, crater walls with inward slumping and outer zones having inward faulting (Kumar, 2005). Based on albedo and surface texture, lunar surface is divided into highlands and mares. The craters present in the mare region are rich in iron-bearing silicate minerals like

olivine and pyroxene. The craters in the highland region shows the abundance of anorthosite material (e.g., plagioclase which is high in alumina and low in iron) (Pieters, 1978). The highland region has higher density of craters than the mare region (McFadden *et al.,* 2006).

The equatorial transition region consists of craters with both the kinds of material deposition i.e. from highland and mare region. The crater highlights distinct morphological features such as Central mound, smooth floors, mare deposits, secondary craters, highland material availability and fracture features (Thaker *et al.,* 2020). This paper focuses on the detailed analysis of crater morphology and mineralogy and finally drawing unique features within the crater.

Study Area

Cavalerius crater is a complex crater lying in between the transition zone of the mare and highland region in the Western Procellerum centred at 5.1°N and 66.8°W (Fig. 1.1 (a)). The diameter of crater varies with the maximum in north-south direction (64.93 Km) and minimum towards the west-east direction (58.49 km). Hence, it is asymmetrical in north-south direction.

Figure 1.1 (c) highlights the distinct morphological features using the crater profile graph. It includes terrace features, smooth floor, central mound and a secondary crater in between central mounds. The rim of the crater is relatively high and it is varying in all directions. The rim to floor relief is maximum in the south direction which is 6 km and minimum in the north, i.e. 5 Km. The LOLA data as shown in figure 1.1 (b) revealed that wall terrace closest to the crater rim is at depth of 1.2 km± 0.1 km in the north and in the east at depth of 0.8 km ± 0.1 km. The western region displays the depth of about 0.5 km ± 0.1 km and the southern region shows 2 km ± 0.1 km wall terrace and closest rim depth.

Materials and Methods

A number of datasets were combined using the ArcGIS software to study the morphology of the basin. Lunar Reconnaissance Orbiter Camera- Wide Angle Camera (WAC) having a uniform resolution of 100m/pixel and Lunar Reconnaissance Orbiter Camera- Narrow Angle Camera (NAC) with 0.5m/pixel resolution (Tschimmel *et al.,* 2009) has been used for the detailed study of a morphology of Cavalerius crater on the moon (Robinson *et al.,* 2010). LROC- NAC images were used to study the different geological feature on the crater floor such a central mound, hummocky floor etc. Lunar Orbiter Laser Altimeter (LOLA) global Digital Elevation Model (DEM) with spatial resolution 30 m/ pixel was used to study the topographic profile of the crater floor (Li *et al.,* 2015). LOLA is a payload on the Lunar Reconnaissance Orbiter (LRO) designed to characterize different morphological features on the Moon (Smith *et al.,* 2010).

The mineral profiling was carried out using Chandrayaan-1 Moon Mineralogy Mapper (M3) level 2 hyperspectral data (Varatharajan *et al.,* 2014).
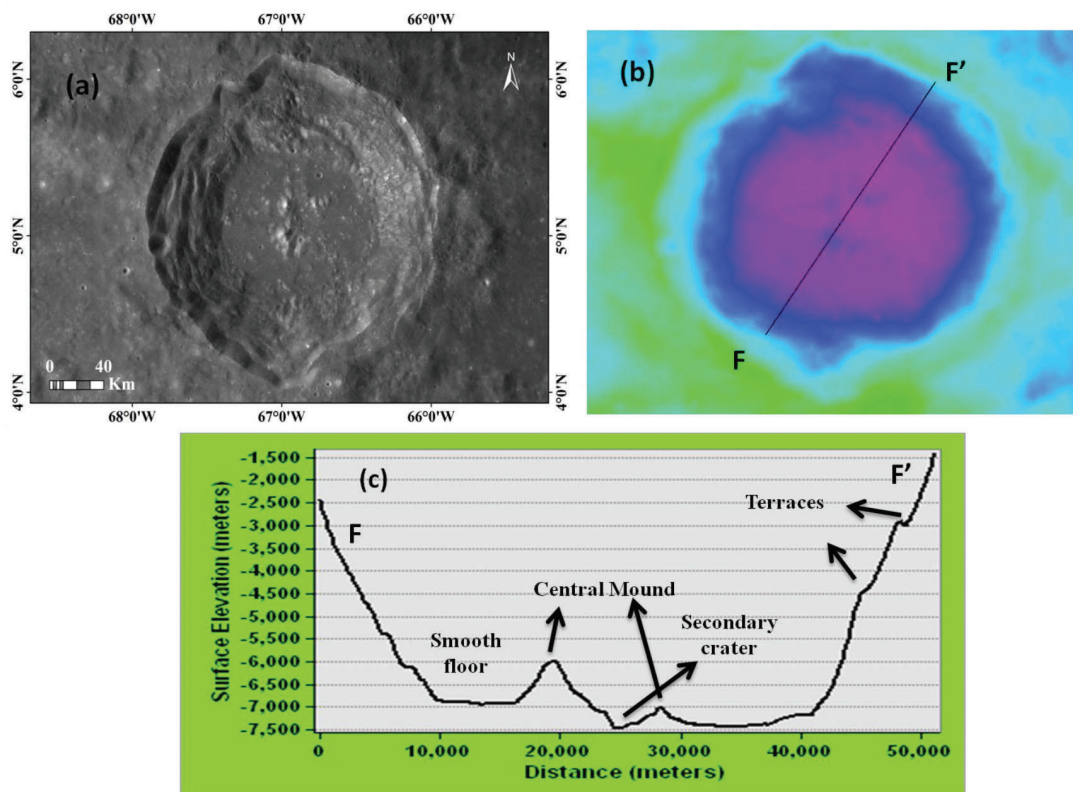

Fig. 1.1 (a) LROC-WAC image of Cavalerius crater. (b) LOLA image of crater with segment FF'. (c) Crater profile graph of segment FF' showing unique morphological features on crater floor.

M3 has the spectral range from 430-3000 nm over 85 spectral channels. The level 2 data product is the reflectance data derived from level 1B radiance data which was calibrated to reduce the noise and artefacts in the dataset. The level 2 data (M3G20090613T161036_V01_RFL) was used to assess the spectral properties of all the geological units present. ENVI-4.7 image processing software was used to perform the mathematical operations of M3 data and generating RGB composite. Integrated band depth (IBD) was calculated at 1 µm and 2 µm using band math function in ENVI. The IBD is a parameter to study lunar mineralogy which combines the band depths over the spectral subset of an absorption feature and is directly proportional to the band area (Varatharajan *et al.*, 2014). In this study, for 1 µm absorption feature continuum endpoints at 699 nm and 1578 nm and for 2 µm absorption feature the continuum endpoints at 1578 nm and 2538 nm were anchored (Varatharajan *et al.*, 2014). The Clementine's multispectral data in the ultraviolet/visible (UV/VIS) and near-infrared (NIR) spectral ranges were used for mineralogical study. It consists of 11 bands having wavelengths 415 nm, 750nm, 900 nm, 950 nm, 1000 nm, 1100 nm, 1250 nm, 1500 nm, 2000 nm, 2620 nm and 2792 nm respectively. The mineral study was carried out using both Clementine and chandrayaan-1 M3 datasets in ENVI-5.2 software. For Clementine data, band strength, band curvature and band tilt were calculated using wavelength 750 nm, 900 nm and 1000nm and RGB colour was assigned to each respectively.

Results and Discussion

Geomorphology of Cavalerius Crater

The Cavalerius crater consists of unique morphological features like a central mound, hummocky unit, terraced rim, Secondary craters and smooth floors.

Figure 1 shows hummocky floor in the north, east and south-east region of the crater floor. It is dominated by isolated mounds which show higher albedo than the surrounding terrain. The average area covered by these isolated mounds measures around 0.9 km2; however, some are as large as 24.63 km2. The crater consists of a mass of two irregular central mounds as shown in figure 1.2. The central mound spread in the west has an elevation of 1 km from the crater floor (figure 1.1(c)). The other central mound
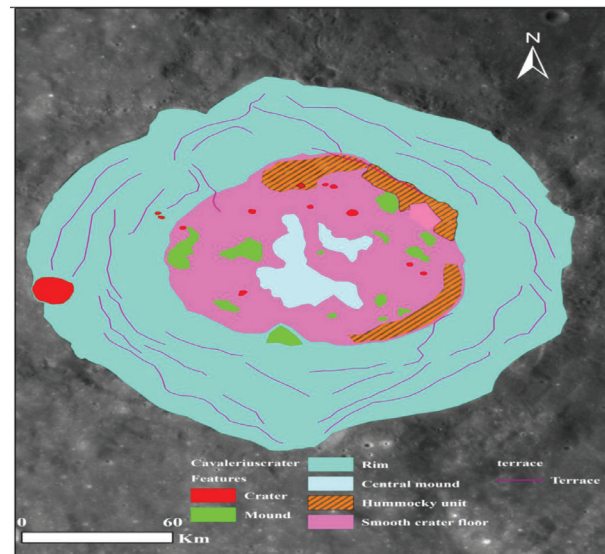

Fig. 1. Morphological map of Kopff crater using base map of LROC-WAC image.

has an elevation of about 0.4 km from the floor. On both the side of central mounds, lies the smooth floor which highlights that the smooth floor in the eastern side of crater floor has more depth than the western side of Cavalerius (figure 1.1 (c)). This might be due to the reason that crater lies in the transition region and part falling on the mare region bears more depth than the region lying in the highland region. The crater has multiple tiers of wall terraces as shown in Figure 1.2. The most prominent wall terraces are seen in the east and west region of the inner rim. The western portion of the crater has 7-8 well-developed terraces, compared to 3-4 terraces in the eastern (mare) portion. The well-developed terraces (marked in black arrows) can be seen in Figure 1.3 (f).

The boulders marked in black arrows in figure 1.3 (a) are present around the central mound in the west which might be due to the erosion of central mound. Figure 1.3 (b) shows isolated mounds on the hummocky units. These mounds are interpreted to be covered with a thin layer of veneer which cooled down rapidly resulting in the formation of wavy like features on the surface as marked in black arrows in figure 1.3 (b). Cone-like features are observed on the smooth floor in west marked in the black circle as shown in Figure 1.3 (c). The inner rim wall in the north has a landslide feature formed as a result of slumping of wall material (Figure 1.3 (d)).
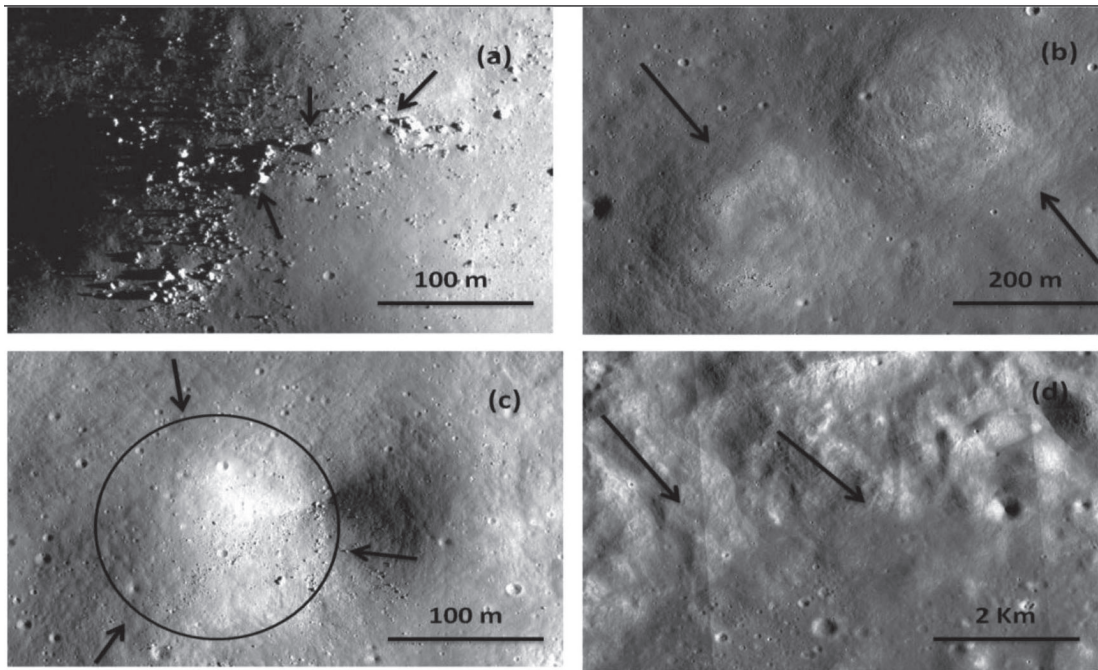
The eastern region of crater floor has flow fea-

Fig. 1.3 (a) LROC NAC image (M1108718339RC) of boulders present near the central mound. (b) Isolated mounds around hummocky unit present in the east studied using LROC-NAC image (M1302882586LC). (c) LROC-NAC image (M1108718339RC) showing cone features in the smooth floor region marked in elliptical circle. (d) LROC-NAC image (M1169963503LC and M1169963503RC) of region showing landslide feature in the north inner rim.

tures (marked in black arrows) in the form of channels indicating the role of melt rich ejecta in its formation. These continuous ejecta channels (Figure 1.3 (e)) or lobes spread in all direction ending up on the hummocky unit in the east.

Mineralogy of Cavalerius Crater

Cavalerius crater present in the transition region in between mare and highland has unique mineralogi-

cal characteristics. Figure 2.1 (a) shows false colour composite generated using integrated band depth method on Chandrayaan-1 M3 data. The inner and outer crater rim and central mound region highlighted in blue colour has stronger band strength value and shows the presence of orthopyroxene. The smooth crater floor emphasizes on the availability of olivine and clinopyroxene (stronger band tilt) marked in green colour.
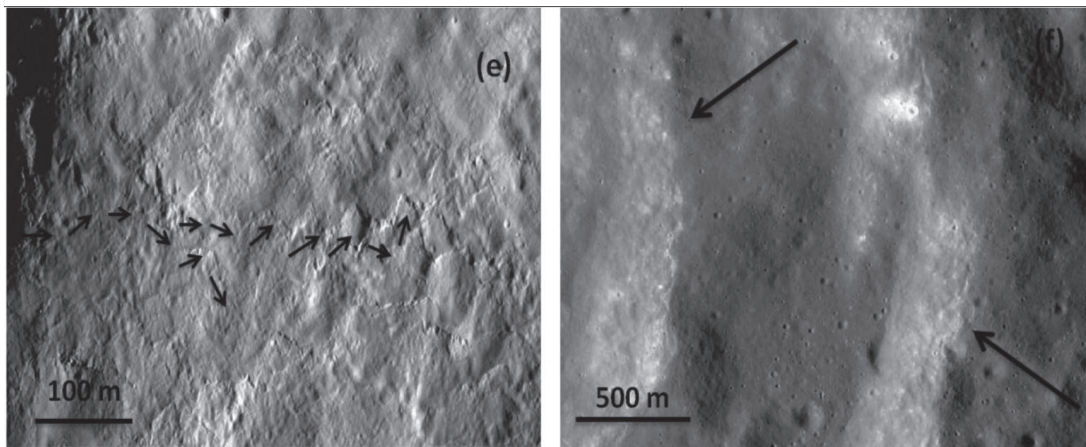

Fig. 1.3 (e) LROC-NAC image (M1136989497LC, M1136989497LC) of melt rich ejecta flowing in the smooth floor region of crater. (f) Terrace features in the east direction studied using LROC-NAC image (M1221741702LC).

Figure 2.1 (b) shows false colour composite image calculated using band ratio parameters of spectral wavelengths in Clementine UVVIS dataset. The region around the crater floor has low calcium pyroxene marked in red colour having high band curvature values. The blue colour region in the inner rim have high band strength value which shows deposition of weathered soil that might be the result of space weathering of surface rocks. Figure 2.1 (c) and (d) highlights the normal and continuum removed spectral graphs of R1 region with olivine abundance (Figure 2.1 (a)) having spectral absorption band 1000 nm.

Five spectral units (Figure 2.1 (a)) were taken after IBD calculation which covered crater floor in the north (R1), region close to central mound (R2), smooth floor in the south (R3), around the secondary crater on the inner rim in west (R4) and smooth floor region in the east (R5).

Band Strength

Figure 2.2 represents the normal and continuum-removed mean reflectance spectra of different units in crater. The mean spectra of all the units show that band 1 is comparatively equivalent to band 2 (except for R4). The band 2 of R4 is broader and stronger due to the presence of spinel on the surface (Table 1). The average albedo of spectral units is found to vary from maximum of 14% in R2 and R3 to a minimum of 10% in unit R1.

Band Centre

The observed band centre values for the spectral units ranged from 950-1009.9 nm for band 1 and 1978.09- 2297.87 nm for band 2 respectively (Table 2).

Figure 2.3 (a) shows BC-BC plot (x-axis BC2 and Y-axis BC1) in which band centre features are used to identify the presence of orthopyroxene, clinopyroxene and intermediate calcium containing pyroxene (Varatharajan *et al.,* 2014). The graph shows three data points towards the top right corner interpreted to be clinopyroxene and those in between the graph to be pyroxene with intermediate calcium.
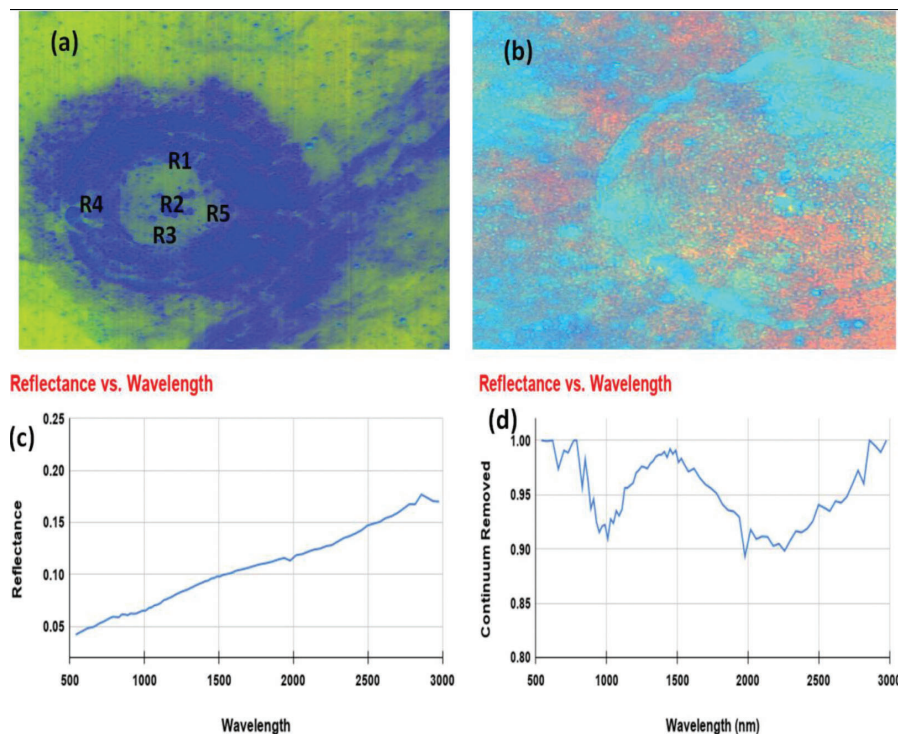

Fig. 2.1 False colour composite (FCC) image of crater generated using chandrayaan-1 M3 label-2 reflectance data (M3G20090613T161036_V01_RFL) The crater highlights five spectral units for the wavelength-reflectance study. (b) FCC image of crater studied using Clementine UV-VIS dataset. (c), (d) Normal and Continuum removed reflectance of the spectral unit R1 (Fig. 2.1 (a)) showing absorption at 1000 and 2000 nm, which indicates pyroxene presence.
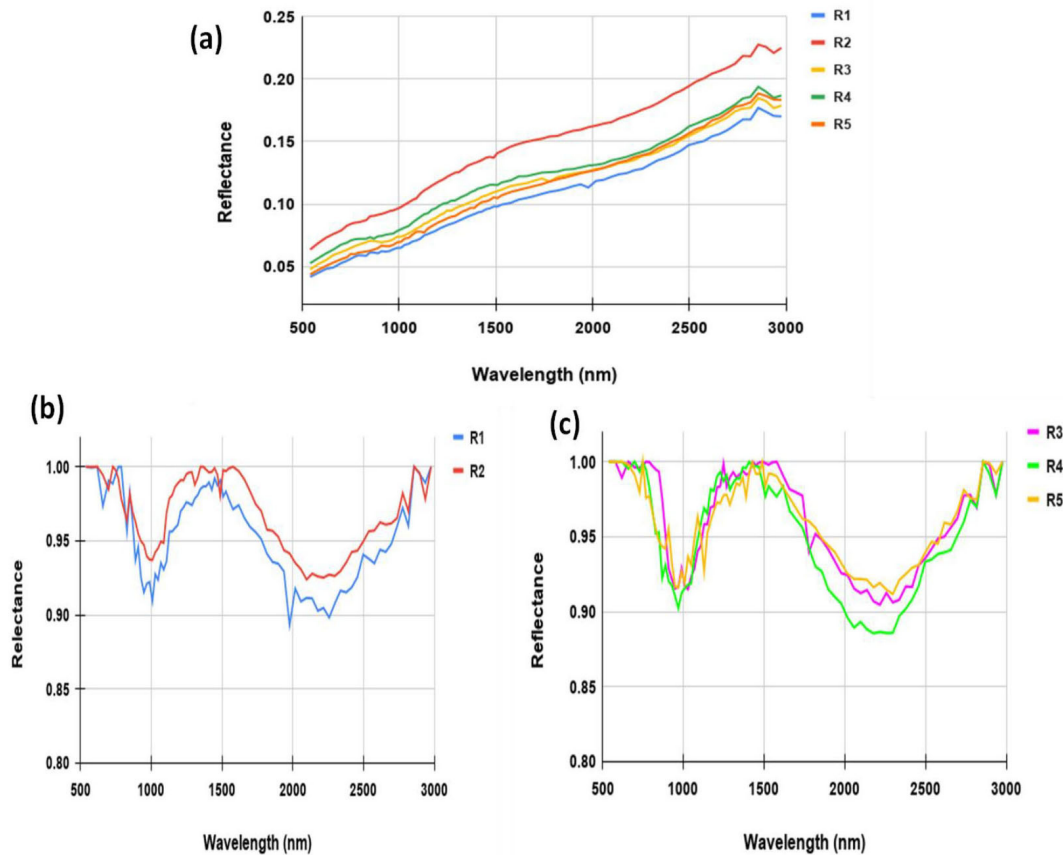
Fig. 2.2 (a) Normal Spectral Reflectance graph. (b) and (c) Continuum Removed Spectral Reflectance of all the spectral units respectively.

Table 1. Details of Band Strengths of mean Spectra of five spectral units.

Spectral units	Reflectance at 1.578 μm	Band 1 Strength (%)	Band 2 Strength (%)
R1	0.101	10	10
R2	0.14	7	7
R3	0.11	9	9
R4	0.11	10	12
R5	0.109	9	8

Table 2. Band Centre values of spectral units.

Spectral Units	Band Centre 1 (nm)	Band Centre 2 (nm)
R1	1009.95	1978.09
R2	1009.95	2097.87
R3	950.05	2297.48
R4	970.02	2297
R5	950.05	2297

Band Area Ratio

Table 3 shows BAR values of all the spectral units which emphasizes on the presence of pyroxene mineral. Higher the BAR value, more the presence of pyroxene mineral (Kaur *et al.*, 2013) (Issacson *et al.*, 2011).

The plot of band 1 centre and BAR values indicates the presence of olivine (OL), pyroxene (BA) and clinopyroxene-olivine mixture (OC) (Varatharajan *et al.*, 2014). Figure 2.3 (b) shows all the data points clustering around the OC region in-

Table 3. Band Area Ratio values for Spectral units.

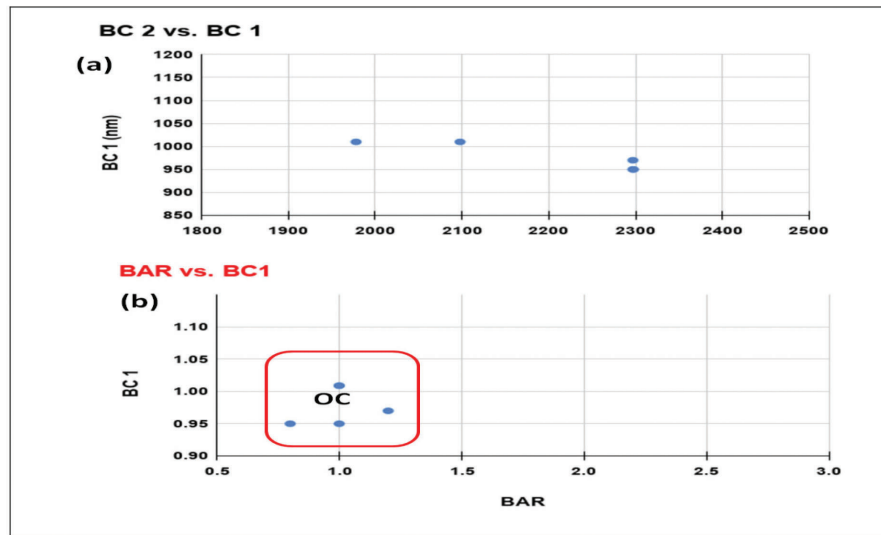| Spectral units	Band Area Ratio
R1	1
R2	1
R3	1
R4	1.2
R5	0.8

Fig. 2.3 (a) Band II centre versus band I centre scatter plot. (b) Band Area Ratio (BAR) versus band I center plot.

dicating the presence of clinopyroxene-olivine mixture.

Discussion

The complex cavalerius crater in the transition equatorial region projects unique morphological characteristics. The crater shows two central mounds in the form of a mass of irregular mound, hummocky floor in the north, east and south-east region, multiple wall terraces and smooth floor unit with different thickness in the east and west directions are morphological units observed in the crater. The smooth floor units are found to have depositions of thin layer of veneer appearing in the form of wavy structure. The inner rim in the north shows that landslide features in the form of slumped wall.

In this study, we have presented a detailed description of the mineralogy of Cavalerius crater based on IBD generated using Chandrayaan-1 M3 level-2 dataset. A total of five spectral units were selected based on spectral variations in the IBD composites. The spectral units displaying green to yellowish-green colour within the crater confirmed the presence of mineral olivine and clino-pyroxene. The blue coloured region in the IBD hue shows deposition of feldspathic material of low mafic content. The crater floor was found to have clino-pyroxene and Olivine while the terraces, inner rim and outer rim had ortho-pyroxene depositions. Band strength was calculated for all the spectral units and it was found that the band 1 and band 2 were comparatively equivalent for all the units except R4. The

BAR Vs BC plot was calculated and it was interpreted that the units belonged to clinopyroxene-olivine (OC) region. The Clementine data studied showed the presence of weathered soil that might have been the material from the highland region. This way crater highlighted the availability of the material from both highland and mare region.

References

Arivazhagan, S. and Karthi, A. 2018. Compositional and chronological characterization of mare crisium using Chandrayaan-1 and LROC-WAC data. *Planetary and Space Science*. 161 : 41-56.

Heiken, G. H., Vaniman, D. T. and French, B. M. 1991. Lunar sourcebook-A user's guide to the moon. *Research supported by NASA. Cambridge, England, Cambridge University Press, 1991, 753 p. No individual items are abstracted in this volume.*

Isaacson, P. J., Pieters, C. M., Besse, S., Clark, R. N., Head, J. W., Klima, R. L. and Taylor, L. A. 2011. Remote compositional analysis of lunar olivine-rich lithologies with Moon Mineralogy Mapper (M3) spectra. *Journal of Geophysical Research: Planets*. 116(E6).

Kaur, P., Bhattacharya, S., Chauhan, P. and Kumar, A. K. 2013. Mineralogy of Mare Serenitatis on the near side of the Moon based on Chandrayaan-1 Moon Mineralogy Mapper (M3) observations. *Icarus.* 222(1) : 137-148.

Kumar, P. S. 2005. Structural effects of meteorite impact on basalt: Evidence from Lonar crater, India. *Journal of Geophysical Research: Solid Earth.* 110(B12)

Li, B., Ling, Z., Zhang, J., Chen, J., Wu, Z., Ni, Y. and Zhao, H. 2015. Texture descriptions of lunar surface derived from LOLA data: Kilometer-scale roughness

and entropy maps. *Planetary and Space Science*. 117 : 303-311.

McFadden, L. A., Johnson, T. and Weissman, P. (Eds.). 2006. *Encyclopedia of the Solar System*. Elsevier.

Papike, J. J. 1998. Lunar samples. *Planetary Materials, 5*.

Pieters, C. 1978. Mare basalt types on the front side of the moon-A summary of spectral reflectance data. Paper presented at the Lunar and Planetary Science Conference Proceedings.

Robinson, M. S., Brylow, S. M., Tschimmel, M., Humm, D., Lawrence, S. J., Thomas, P. C. and Caplinger, M. A. 2010. *Lunar reconnaissance orbiter camera (LROC) instrument overview.* Space Science Reviews. 150(1-4): 81-124.

Smith, D. E., Zuber, M. T., Neumann, G. A., Lemoine, F. G., Mazarico, E., Torrence, M. H. and Aharonson, O. 2010. Initial observations from the lunar orbiter laser altimeter (LOLA). *Geophysical Research Letters*. 37(18).

Thaker, A. D., Patel, S. M. and Solanki, P. M. 2020. Morphological analysis and mapping of complex craters of Copernican age: Crookes, Ohm and Stevinus. *Planetary and Space Science.* 184 : 104856.

Tschimmel, M., Robinson, M. S., Humm, D. C., Denevi, B. W., Lawrence, S. J., Brylow, S. and Ghaemi, T. 2009. March). Lunar Reconnaissance Orbiter Camera (LROC): Ready for rocks. In: *Lunar and Planetary Science Conference* (Vol. 40).

Varatharajan, I., Srivastava, N. and Murty, S. V. 2014. Mineralogy of young lunar mare basalts: Assessment of temporal and spatial heterogeneity using M3 data from Chandrayaan-1. *Icarus*. 236 : 56-71.